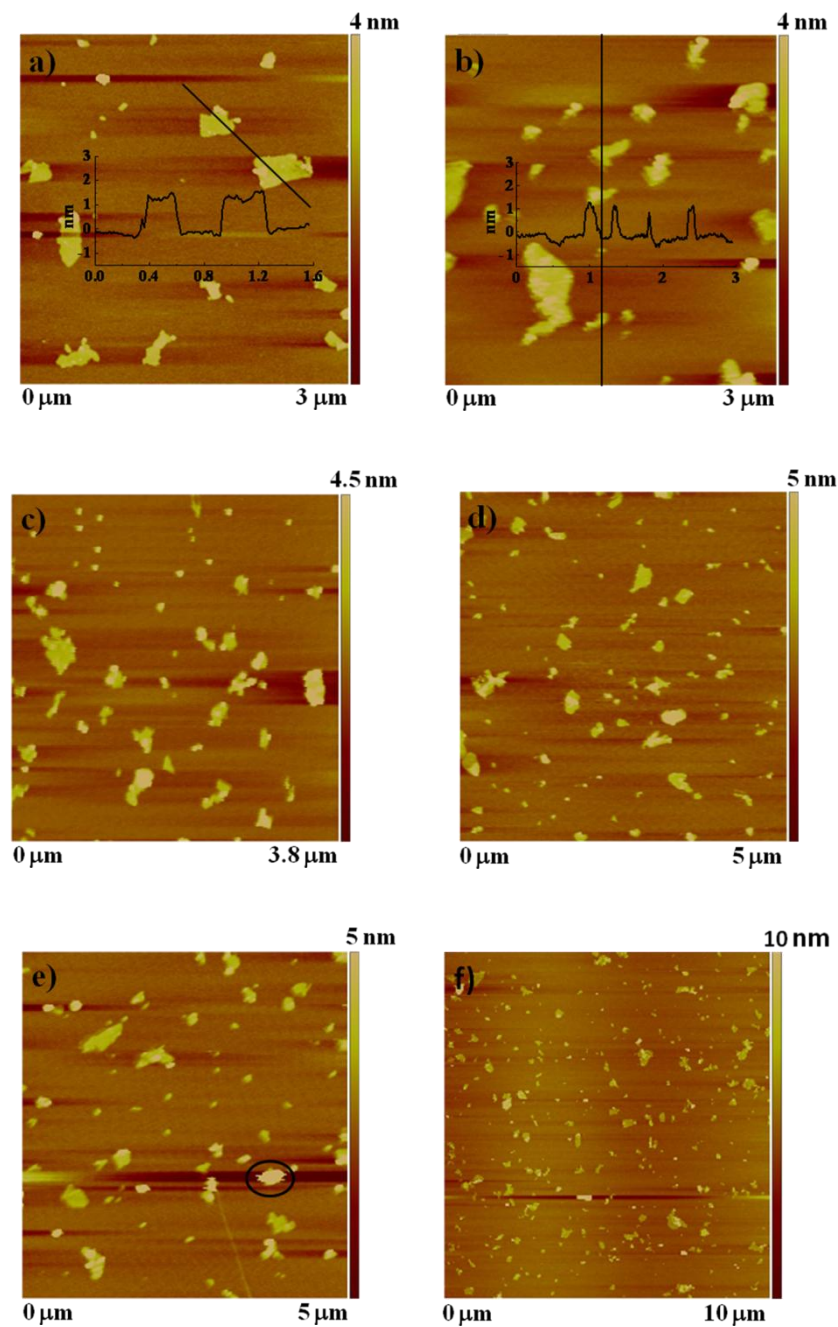


## Supplementary Information

### Understanding the Relationship of Performance with Nanofiller Content in the Biomimetic Layered Nanocomposites

*Jianfeng Wang, Qunfeng Cheng,\* Ling Lin, Linfeng Chen and Lei Jiang*



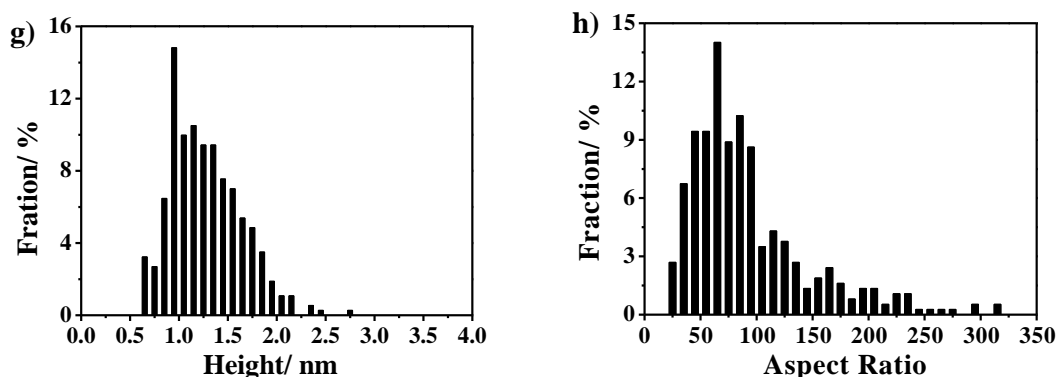


Fig. S1 (a-f) AFM images of MMT platelets deposited on mica. (g) The distributions of mean height. (h) The distributions of mean aspect ratio. The results show that the average mean thickness and average aspect ratio of MMT platelets are  $1.28 \pm 0.36$  nm and  $93 \pm 54$ , respectively.

For AFM imaging, the prepared MMT suspension (0.31 wt%) was diluted with acetone to  $1 \times 10^{-3}$  wt%. The diluted suspension (10  $\mu$ L) was dropped onto a freshly cleaved mica disk (12.5 mm in diameter) and dried at room temperature. The typical AFM images were shown in Fig. S1a-f. The obtained images were analyzed using the Scanning Probe Image Processor (SPIP) image analysis software (Image Metrology). Through the SPIP image analysis, the mean height and lateral area of every MMT platelet can be obtained. During analysis, the particles with lateral area less than 1500  $\text{nm}^2$  or thickness less than 0.6 nm were excluded. A few particles are obviously much too tall to be platelets (e.g., the highlighted particle in Fig. S1e) were observed occasionally. They are presumably residual mineral contamination.<sup>1</sup> So, they were excluded from the analysis. Fig. S1g gives the distribution of the mean height of MMT platelets. The distribution shows that the average mean height is 1.28 nm with a standard deviation of 0.36 nm ( $N = 371$ ). This value agrees well with that of XRD result (1.26 nm) and slightly higher than the theoretical thickness of a single platelet (1.0 nm).

For platelet having irregular shapes, the aspect ratio ( $s$ ) is defined as the ratio of square root of platelet lateral area ( $A$ ) to thickness ( $t$ ),

$$s = \frac{\sqrt{A}}{t} \quad (1)$$

For each platelet, the lateral area and mean thickness are known from SPIP analysis. Compiling the aspect ratio of all platelets in 9 images produces the aspect ratio distribution. The aspect ratio distribution is shown in Fig. S1h. From this distribution, we find that the average aspect ratio is 93 and the standard deviation is 54.

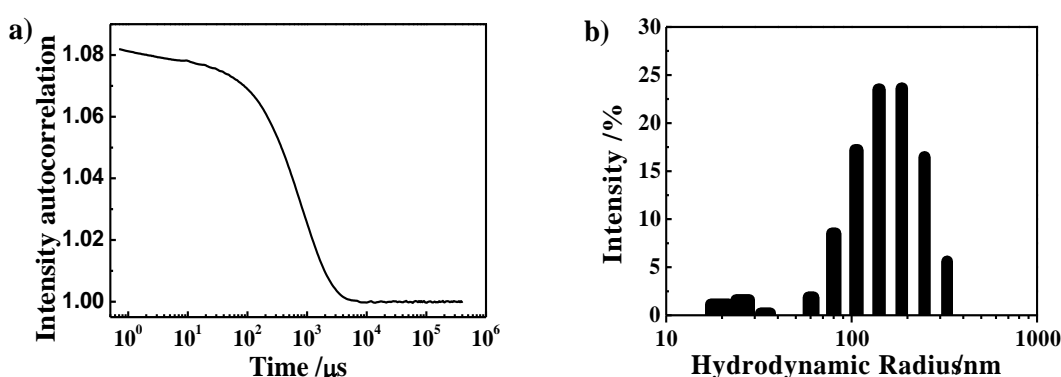


Fig. S2 (a) Autocorrelation function from DLS measurement for dilute MMT dispersion in water. (b) The distribution of the apparent hydrodynamic radius of MMT nanoplatelets from regularization analysis.

Although DLS cannot measure degree of exfoliation and the aspect ratio of MMT, it provides a convenient, fast method to obtain an effective hydrodynamic diameter of an equivalent sphere. Regularization analysis of autocorrelation function was carried out to generate the distribution of MMT sizes, as shown in Fig. S2b. the distribution displays a predominant peak and a minor peak. The predominant peak reveals particles with an average hydrodynamic radius of 167.9 nm, indicating the absence of MMT aggregates.<sup>2</sup> In general, the hydrodynamic diameter of MMT nanoplatelets is larger than the diameter measured by AFM.<sup>1</sup>

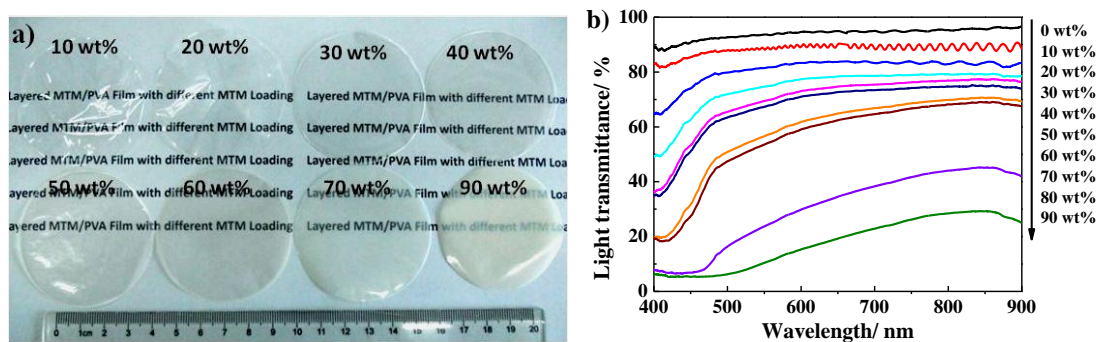


Fig. S3 (a) Photograph and (b) Light transmittances of MMT/PVA composite films with different MMT content. Thicknesses of the films are about 7–9  $\mu\text{m}$ .

The films are transparent, smooth and glossy. The light transmittance of the films gradually decreases with MMT content due to light scattering by the MMT nanoflatelets. High transparency is basically maintained for 30-70 wt% MMT content. However, the 80 wt% and 90 wt% MMT/PVA nanocomposites exhibit obviously lower transparencies, probably because of inhomogeneity arising from tactoids, proved by XRD (Fig. S4).

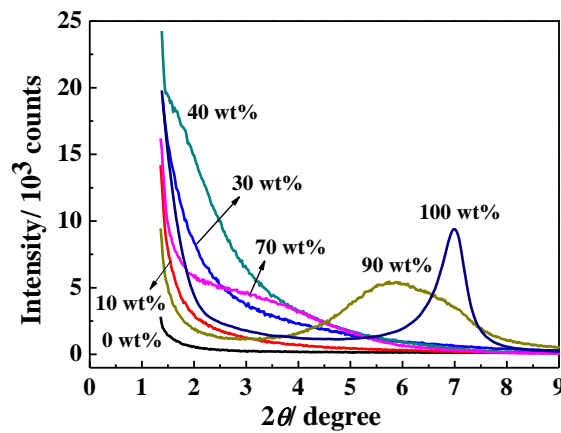


Fig. S4 XRD of the MMT/PVA nanocomposites with different MMT content. It reveals that the state of dispersion of MMT changes from exfoliated to intercalated state, then to tactoids with the increase of clay loading.

Pure MMT film has a prominent basal reflection at  $2\theta = 7^\circ$ , corresponding to a  $d$  spacing of 1.26 nm. For 10 wt% filler content, a featureless profile devoid of peaks is

shown. Furthermore, the intensity is lower than MMT. These suggest that the majority of MMT is exfoliated. In contrast, higher diffraction intensity than MMT in the range of  $1.5^\circ$  to  $5.2^\circ$  is observed as MMT content is between 30 wt% and 70 wt%, indicating the existence of intercalated structure with  $d$  spacing below 5.8 nm. The  $d$  spacing for 70 wt% MMT/PVA film calculated from the broad reflection at  $2\theta = 3.8\text{--}5.2^\circ$  is about 1.7-2.2 nm. Distinctively, 90 wt% MMT/PVA film exhibits a broad peak, which partly overlaps the peak of pure MMT. This suggests that partial MMT platelets are restacked and form tactoids, probably because the PVA is too little to fully cover all of the MMT platelets.

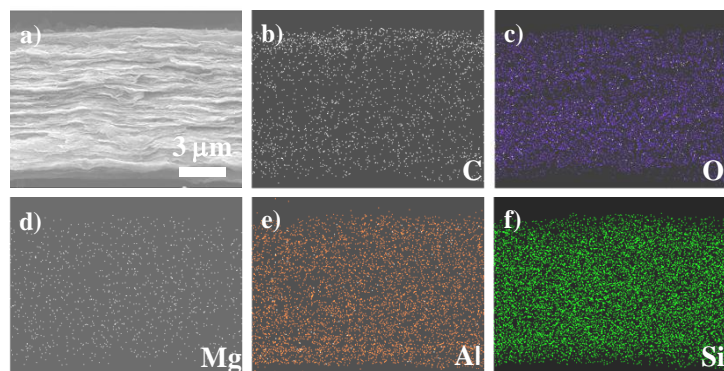


Fig. S5 (a) SEM image of the cross section and (b-f) corresponding EDX mapping of the different components in 70 wt% MMT/PVA composite, revealing that PVA and MMT are both homogeneously distributed, without aggregation. (b) Carbon originating from PVA, (c) oxygen originating from MMT and PVA, (d) magnesium originating from MMT, (e) aluminum originating from MMT, and (f) silicon originating from MMT.

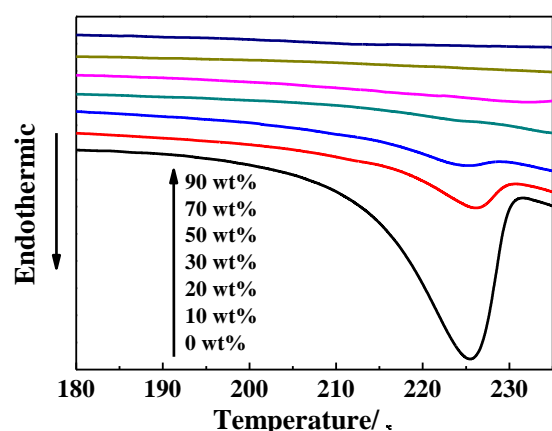


Fig. S6 DSC curves of MMT/PVA nanocomposites, showing increasing suppression of the thermal motion of the PVA chains with MMT content.

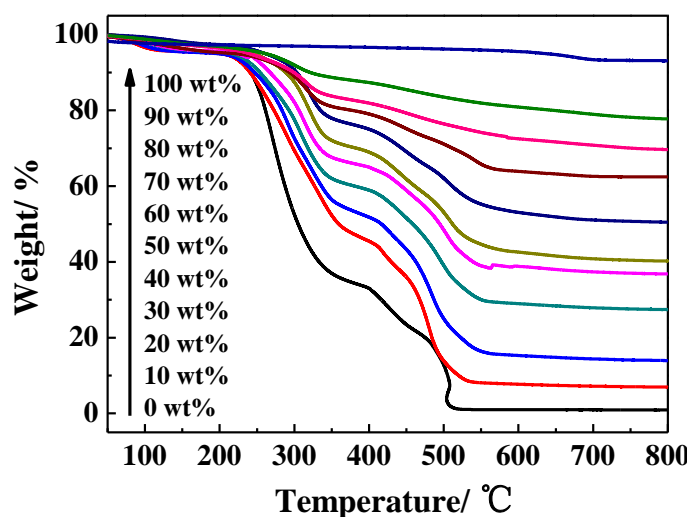


Fig. S7 TGA curves of PVA/MMT nanocomposites with varying MMT mass content.

Table S1 The parameters obtained from DSC, and calculated volume fraction of MMT from the densities of MMT and PVA.

Sample	$\phi$ [vol%]	$T_m$ [°C]	$\Delta H_m$ [J g <sup>-1</sup> ]	$X_c$ [%]	$T_{onset}$ [°C]
Pure PVA	0	225.5	59.0	42.6	243
10 wt% MMT/PVA	4.7	226	19.6	15.2	239
20 wt% MMT/PVA	10.0	225.5	6.0	5.0	253
30 wt% MMT/PVA	16.0	—	0	0	260
40 wt% MMT/PVA	22.8	—	0	0	270
50 wt% MMT/PVA	30.7	—	0	0	281
60 wt% MMT/PVA	40.0	—	0	0	288
70 wt% MMT/PVA	51.0	—	0	0	285
80 wt% MMT/PVA	64.0	—	0	0	275
90 wt% MMT/PVA	80.0	—	0	0	264
Pure MMT	100	—	0	0	> 800

The degree of crystallinity ( $X_c$ ) of PVA was calculated as follows:

$$X_c = \frac{\Delta H_m}{\Delta H_0 \times (1-w)} \times 100\% \quad (2)$$

where  $\Delta H_m$  is the measured melting enthalpy of nanocomposites from DSC and  $\Delta H_0$  is the enthalpy of 100% crystalline PVA ( $138.6 \text{ J g}^{-1}$ ).<sup>3,4</sup>  $w$  is the weight fraction of MMT in composites obtained from TGA results.

The weight fraction of MMT of composites is transformed into volume fraction from

$$\phi = \frac{w/\rho_f}{w/\rho_f + (1-w)/\rho_m} \quad (3)$$

where  $w$  is the weight fraction of MMT in composites and  $\rho_f$  and  $\rho_m$  are the densities of MMT ( $2.86 \text{ g cm}^{-3}$ ) and PVA ( $1.269 \text{ g cm}^{-3}$ ), respectively.

The theoretical prediction from Padawer-Beecher and shear lag models

For platelet-reinforced nanocomposites, the Padawer-Beecher can be used to predict the composite Young's modulus ( $Y$ ).<sup>5</sup> The Padawer-Beecher model gives the composite modulus to be

$$Y = \alpha \phi_f Y_f + (1 - \phi_f) Y_m \quad (4)$$

Where  $Y_f$  and  $Y_m$  are the Young's modulus of platelet and polymer matrix, respectively, and  $\alpha$  is the aspect ratio effective factor.  $\alpha$  is defined as

$$\alpha = 1 - \frac{\tanh(u)}{u}$$

The  $u$  reads

$$u = s \sqrt{\frac{G_m \phi_f}{Y_f (1 - \phi_f)}}$$

Where  $s$  and  $\phi$  are the aspect ratio and volume fraction of platelets, respectively, and the shear modulus of polymer matrix,  $G_m$ , is

$$G_m = \frac{Y_m}{2(1+\nu)}$$

For our MMT/PVA systems, the Young's modulus of PVA matrix and MMT platelet are 0.34 and 270 GPa, respectively.<sup>6</sup> The aspect ratio of MMT platelets is 93 (Fig. S1). The Poisson ratio of polymer,  $\nu$ , is 0.5.

The yield strength of platelet-reinforced polymer composites can be predicted by the shear lag model.<sup>7,8</sup> Yield strength of composites ( $\sigma$ ) is given as

$$\sigma = \beta \phi_f \sigma_f + (1 - \phi_f) \sigma_m \quad (5)$$

where  $\sigma_f$  and  $\sigma_m$  are the yield strength of platelet and polymer matrix, respectively. For the fracture case of the platelet pull-out and plastic flow of matrix,  $\beta$  is

$$\beta = \tau_y s / 2\sigma_f$$

For our systems, MMT/PVA nanocomposites with low filler content failed under platelet pull-out mode and PVA matrix generated obvious plastic flow. So, the equation 5 was used to estimate the strength of MMT/PVA composites with MMT content less than 30 wt%. The aspect ratio of MMT platelets is 93 (Fig. S1). Measured yield strength of PVA is 22 MPa. The yield shear strength of PVA,  $\tau_y$ , is taken to be  $\sim 0.5\text{--}0.6\sigma_m$ .

- [1] H. J. Ploehn and C. Liu, *Ind. Eng. Chem. Res.*, 2006, 45, 7025-7034.
- [2] K. Kolman, W. Steffen, G. Bugla-Płoskon'ska, A. Skwara, J. Pigaowski, H. J. Butt and A. Kiersnowski, *J. Colloid Interf. Sci.*, 2012, 374, 135-140.
- [3] F. T. Cerezo, C. M. L. Preston and R. A. Shanks, *Macromol. Mater. Eng.*, 2007, 292, 155-168.
- [4] J. X. Su, Q. Wang, R. Su, K. Wang, Q. Zhang and Q. Fu, *J. Appl. Polym. Sci.*, 2008, 107, 4070-4075.
- [5] G. E. Padawer and N. Beecher, *Polym. Eng. Sci.*, 1970, 10, 185-192.
- [6] O. L. Manevitch and G. C. Rutledge, *J. Phys. Chem. B*, 2004, 108, 1428-1435.
- [7] B. Glavinchevski and M. Piggott, *J. Mater. Sci.*, 1973, 8 1373-1382.
- [8] L. J. Bonderer, A. R. Studart and L. J. Gauckler, *Science*, 2008, 319, 1069-1073.